

## PERFORMANCE OF COPPER NANOFLUID ON CHANGING WIDTH OF STRETCHING SHEET USING THERMAL RADIATION AND HEAT FLUX

by

**Pragya PANDEY<sup>a\*</sup> and Vairavel MADESHWAREN<sup>b</sup>**

<sup>a</sup>Department of Mathematics, SRM IST Ramapuram, Chennai, TamilNadu, India

<sup>b</sup>Department of Mechanical Engineering, Annapoorna Engineering College, Salem, TamilNadu, India

Original scientific paper

<https://doi.org/10.2298/TSCI240215162P>

*The phenomenon of nanomaterial carrying fluid-flow over a non-linear elongated sheet with changing thickness is investigated in this study. The present research focuses at the flow of magnetic nanofluid over non-linear elongated sheets of different thicknesses, with an emphasis on copper nanoparticles distributed in water. The phenomena, which is significant in many industrial applications including paper manufacturing and atomic reactors, is analysed using Prandtl boundary-layer theory and Navier-Stoke's equation. The study covers a wide range of physical features. There have been fewer works on the mathematical modelling of stretching sheets with varying widths. The main aim of investigation is to analyse the effect of EMHD, as well as other characteristics like Eckert number, Boit number, radiation effect, and absorption factor. Paper manufacturing, dye and filament extrusion, atomic reactors, and metallurgical processes all rely heavily on these sheets of varied widths. The problem employs Navier-Stokes' equation and Prandtl boundary-layer theory. The similarity transformation converts PDE into ODE. The MATLAB bvp4c programme is used to obtain numerical solutions. The present study helps to achieve desired quality of stretching sheet.*

Key words: *nanofluid, nanoparticles, stretching sheet, thermal radiation, viscosity, EMHD*

### Introduction

Experts in this field are interested in the study of stretching sheet cooling because of its many potential uses. In numerous industries, different areas of application have initialized the cooling of stretching sheets due to its practical applicability. Although different fluids are used for cooling, but role of nanofluid has upper hand over all other fluids. The fluid-flow over stretching sheet has many applications in industrial phenomenon like manufacturing fibres from glass, extracting polymer sheets, drawing of wire and many more. The quality of processed product depends on rate of heat removal. Many scholars analysed the mode of action of nanofluid in different geometrical fields, like [1] studied nanofluids flow problem past over a stretchable sheet. An exact solution of thin fluid-flow layer exposed to stretching sheet was designed by [2]. The effect of dust particles dispersed in a nanofluid over stretched plate was

---

\*Corresponding author, e-mails: [pragypandeypublication@gmail.com](mailto:pragypandeypublication@gmail.com); [phdannauniv2020@gmail.com](mailto:phdannauniv2020@gmail.com)

explored with different formulation [3]. The flow generated by nanofluid exposed over an exponentially stretchable plate [4] along with effects of viscous dissipation was pondered. The properties of fluid-flow through a vertical plate and their results on phenomenon of heat transfer [5] in a porous media along tiny sized suspensions was published with an innovative technique. The numerical solution of the nanofluid-flow and characteristics of transfer of heat with different types of nanofluids on an elongated surface are of interest and were presented by [6]. The problem of the free convection in a cavity with time period along nano particle based fluid was designed mathematically and solved numerically [7]. The two-phase paradigm by examining the nanofluid with a water base and was customized by [8] to look at the impact of various metal nanoparticle kinds on the clubbed magnetic effect. The effects of dust grains dispersed from a stretched surface was incorporated [9] with flow of nanofluid. Dispersed fluid particles were studied and designed [10] with viscous dissipation past over increasingly stretchy sheet in a magnetic fluid-flow. The comparison between characteristics of heat transfer and fluid-flow quantitatively [11] using different nanofluids on a stretchy surface. The outcome of nanoparticle shape was examined [12] at point of the magneto stagnation flow with effect of chemical reaction as well as thermal radiation. A 3-D magneto stable flow in the space between a disc of nanofluid was created [13] and Casson stimulated by gyrotactic microbes and a cone were solved using the HAM approach. Lately, [14] derived the effect of flow of nanofluid over moving disc with effects of magnetic field. The effect of magnetic field with interpreted convective flow past over an inclined stretched plate with the unsteady thin film flow of nanofluid is examined [15].

The MHD flow in nanofluids has gained importance due to its extraordinary capacity to control the rate of heat transfer. The MHD is mainly derived from three terms: magneto, hydro, and dynamics that were named by [16]. The phenomenon of flow with MHD on a stretched plate up to a stagnation point was introduced [17] and solved numerically the finite difference method. Buongiorno's model was utilized to investigate MHD flow of nanofluid over extending plate with slip conditions [18].

The aforementioned studies as well as the broad use in machine building and industry [19-21] serve as the motivation for the current effort. Additionally, it should be mentioned that studies on heat transmission have made extensive use of linear extending sheets. To account for the importance of electro magneto hydro dynamic (EMHD), a non-linear elastic sheet of varying width has also been simulated along the boundary-layer flow of a nanofluid. Variable-width stretching sheets find practical applications in the metal industry, appliance constructions and patterns, nuclear reactor mechanisation, filament extrusion, paper industry, and several other fields [22-25]. Velocity slip along ternary nanofluid past over stretching sheet was inquired [26] and concluded that inclusion of third nanoparticle enhanced conduction of heat. Hybrid nanofluid over porous stretched sheet was figured [27]. The result was investigated by taking equal proportions of water and ethyl glycol. The dual effect of two particle nanofluid and magnetic field was analysed by [28, 29]. This study aims to calculate the effects of many parameters on nanofluid-flow over a slandering extending plate, including non-linear thermal radiation, changing heat flux, viscous dissipation, EMHD, and ohmic heating.

### Mathematical modelling

A 2-D nanofluid is passed over stretching sheet of changing thickness. The nature of sheet is considered non-linear, fig. 1. The velocity of fluid is given by velocity  $U_w(x) = b(x + c)^n$  where  $b$  is a constant,  $c$  is the parameter of extension, and  $n$  is the exponential parameter. Direction of stretching plate is taken as  $X$ -axis. The EMHD is considered along  $Y$ -axis. The

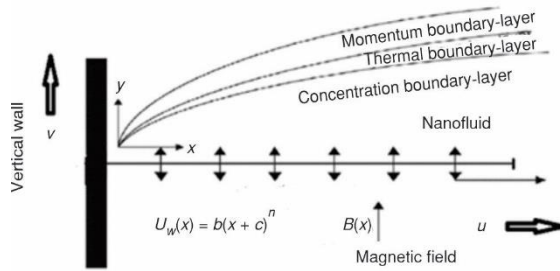


Figure 1. Three different boundary-layer

variation of thickness is taken as  $y = N(x+c)(1-n)^2$ . It is assumed that pressure difference does not change the length of the stretching sheet. The  $N$  is a taken minor factor for this purpose. Application of two forces of equal magnitude and opposite direction leads to elongation of plate through its slit.

For keeping Reynolds' number in low range we apply electric and magnetic field perpendicular to direction of flow. The equations for electric and magnetic field is given by field  $E(x) = E_0(x+c)^{(n-1)/2}$

and  $B(x) = B_0(x+c)^{(n-1)/2}$ , respectively. Temperature difference within layers of fluids is neglected. Furthermore, effects of viscous dissipation, non-uniform heat flux, and Joule heating are taken into account and incorporated with energy equations:

$$\frac{\partial u}{\partial x} + \frac{\partial v}{\partial y} = 0 \quad (1)$$

$$\rho_{nf} \left( u \frac{\partial u}{\partial x} + v \frac{\partial v}{\partial y} \right) = \frac{\partial}{\partial y} (\mu(T)) + \frac{\sigma_{t,nf} B_o^2 u}{\rho_{t,nf}} + \sigma_{nf} (E(x)B(x) - B(x)^2 u) \quad (2)$$

$$(\rho C)_{nf} \left( u \frac{\partial T}{\partial x} + v \frac{\partial T}{\partial y} \right) = k_{nf} \frac{\partial^2 T}{\partial y^2} + \frac{16\sigma^*}{3k^*} \frac{\partial^2 T}{\partial y^2} + \mu_{nf} \left( \frac{\partial u}{\partial y} \right)^2 + q''' + \sigma_{nf} (uB(x) - E(x))^2 \quad (3)$$

Along with boundary conditions in eq. (4):

$$u = U_w(x) = b(x+c)n, v = 0, -k \frac{\partial T}{\partial y} = h(T_w - T) \text{ at } y = N(x+c)^{n-1/2} \text{ and } y \rightarrow \infty, u \rightarrow 0, T \rightarrow T_\infty \quad (4)$$

where the elements of speed along co-ordinate axes are denoted by  $u$  and  $v$ ,  $T$  – the temperature fluid temperature,  $\rho_{nf}$  – the density,  $\sigma_{nf}$  – the measure of electrical conduction,  $\sigma^*$  – the coefficient given by Stefan-Boltzmann, and  $k^*$  – the average value of absorption. The value of coefficient of viscosity [17] is given by:

$$\mu(T) = \mu^* [a_1 + b_1(1-\theta)(T_w - T_\infty)] \quad (5)$$

where  $\mu^*$  is the standard value for reference of viscosity whereas  $a_1, b_1$  are constants. The  $q'''$  denoted in third equation denotes the non-uniform value of flux and is calculated from eq. (5):

$$q''' = \frac{k_{nf} U_w(x)}{v_f(x+c)} [A^* (T_w - T_\infty) + B^* (T - T_\infty)] \quad (6)$$

where  $A^*$  and  $B^*$  are parameter of heat flux which is dependent on time.

### Conversion of equations

To solve the given PDE, dimensionless variables (7)-(11) are introduced:

$$\psi = (b\mathcal{G}_{nf})^{1/2} xf'(\eta) \quad (7)$$

$$\eta = \left( \frac{(n+1)b(x+c)^{n-1}}{2\mathcal{G}} \right)^{1/2} y \quad (8)$$

$$u = b(x+c)^n f'(\eta) \quad (9)$$

$$v = - \left( \frac{(n+1)b(x+c)^{n-1}}{\mathcal{G}} \right)^{1/2} \left( f(\eta) + \eta f'(\eta) \frac{n-1}{n+1} \right) \quad (10)$$

$$T = T_\infty + (T_w(x) - T_\infty) \quad (11)$$

where  $\psi(x, y)$  is the streamline function and  $u = \partial\psi/\partial y$  and  $v = -\partial\psi/\partial x$ ,  $\eta$  is the variable of similarity and temperature is non-dimensionalised as:

$$\theta(\eta) = \frac{T - T_\infty}{T_w - T_\infty} \quad (12)$$

It is necessary to convert the PDE to ODE in:

$$A_0 \left[ (a_1 + A(1-\theta)) f''' - A\theta' f'' \right] + A_1 \left[ f''' f - \frac{2n}{n+1} (f')^2 \right] + A_2 M (E_1 - f') = 0 \quad (13)$$

$$\theta'' \left( A_4 + \frac{4}{3} Rd \right) + Pr \left[ A_0 Ec (f'')^2 + A_2 Ec M (f' - E_1)^2 + A_3 f \theta' - A_3 f' \theta \frac{1-n}{1+n} \right] + A_4 \frac{2}{n+1} (A^* f' + B^* \theta) = 0 \quad (14)$$

where  $f(\eta) = (1-n/1+n)\alpha$ ,  $f'(\eta) = 1$ ,  $\theta'(\eta) = \delta[1 - \theta(0)]$  at  $\eta = 0$  and  $f'(\eta) = 0$ ,  $\theta(\eta) = 0$ ,  $\eta \rightarrow \infty$ .

The non-dimensional parameters are given by:

$$M = \frac{2\sigma_f B_o^2}{\rho_f b(n+1)}, E_1 = \frac{E_o}{B_o b(x+c)^n}, Rd = \frac{4\sigma^* T_\infty^3}{kk_f}, Ec = \frac{b^{2(x+c)^2}}{(C_p)_f (T_w - T_\infty)}, Pr = \frac{\mathcal{G}_f (C_p)_f}{k_f}$$

$$\alpha = N \left( \frac{b(n+1)}{2\mathcal{G}_f} \right)^{1/2}, \delta = \frac{h}{k_f} \left( \frac{2\mathcal{G}_f (x+c)}{b(n+1)} \right)^{1-n}, A = b_1 (T_w - T_\infty)$$

where  $M$  is the magnetic field intensity,  $E_1$  – the intensity of electric field,  $Rd$  – the parameter for radiation,  $Pr$  – the Prandtl number,  $Ec$  – the Eckert number,  $\alpha$  – the wall thickness,  $\delta$  – the Biot number, and  $A$  – the variable viscosity parameter.

#### Thermophysical properties of nanofluid:

To compute constant values, the thermophysical properties of water and copper are shown numerically in tab. 1.

**Table 1. Thermophysical parameters**

| Material         | Density, $\rho$ [kgm <sup>-3</sup> ] | $k$ [Wm <sup>-1</sup> K <sup>-1</sup> ] | $\sigma$ [Sm <sup>-1</sup> ] | $C_p$ [Jkg <sup>-1</sup> K <sup>-1</sup> ] |
|------------------|--------------------------------------|---|------------------------------|--|
| H <sub>2</sub> O | 997.1                                | 0.613                                   | 0.05                         | 4179                                       |
| Cu               | 8933                                 | 401                                     | $5.96 \times 10^7$           | 385  |

The volume fraction,  $\phi$ , of nanoparticles used determines the heat capacity, thermal conductivity, and viscosity of the nanofluids. The nanofluid's effective density is determined by:

$$\rho_{nf} = (1 - \phi)\rho_f + \phi\rho_s \quad (15)$$

and heat capacitance of nanofluid:

$$(\rho C_p)_{nf} = (1 - \phi)(\rho C_p)_f + \phi(\rho C_p)_s \quad (16)$$

According to Brinkman (1952), the dynamic permeability of nanofluids is as:

$$\mu_{nf} = \frac{\mu_f}{(1 - \phi)^{2.5}} \quad (17)$$

$$\frac{k_{nf}}{k_f} = \frac{(k_s + 2k_f) - 2\phi(k_f - k_s)}{(k_s + 2k_f) + \phi(k_f - k_s)} \quad (18)$$

The electrical conductivity of nanofluid is given by:

$$\sigma_{nf} = 1 + \frac{3\phi \left( \frac{\sigma_p}{\sigma_f} - 1 \right)}{\left( \frac{\sigma_p}{\sigma_f} + 2 \right) - \left( \frac{\sigma_p}{\sigma_f} - 1 \right) \phi} \sigma_f \quad (19)$$

#### *Skin friction coefficient*

The skin friction coefficient,  $C_f$ , is given by:

$$C_f = \frac{\tau_w}{\rho_f U_w^2} \text{ where } \tau_w = \mu_{nf} \left( \frac{\partial u}{\partial x} \right)_{y=N(x+c) \frac{n-1}{2}}$$

Using we get:

$$C_f \text{ Re}_x^{1/2} = \frac{A_0}{A_4} \left( \frac{n+1}{2} \right)^{1/2} f''(0) \quad (20)$$

#### *Nusselt number*

The concept of the Nusselt number is: Nusselt number for nanofluids is given by:

$$\text{Nu} = \frac{(x+c)q_w}{k_f(T_w - T_f)} \text{ where } q_w = -k_f \left( \frac{\partial T}{\partial y} \right)_{y=N(x+c) \frac{n-1}{2}}$$

Using we get:

$$\text{Nu Re}_x^{-1/2} = -A_4 \left( \frac{n+1}{2} \right)^{1/2} \theta'(0) \quad (21)$$

*Solution of the problem*

Numerical methods are best to solve non-homogeneous equations. The system was converted into  $n$  linear equation. The Adam-Bashforth predictor corrector method was employed for obtaining solution. It is a linear multistep methodology, helps to improve accuracy by using values of last phase.

The process of solving contains two stages, first to get suitable values as a predictor and Adam-Moulton method to get corrector

The first order system for  $\theta(\eta)$  and  $f(\eta)$  is as:

$$f_1 = f', f_2 = f_1', f_3 = f_2' \quad (22)$$

$$f_3 = f_2' = \frac{1}{a_1 + A(1-\theta)} \left[ A\theta_1 f_2 - \frac{A_1}{A_0} (f_2) f - \frac{2}{n+1} (f_1)^2 - \frac{A_2}{A_0} M(E_1 - f_1) \right] \quad (23)$$

$$\theta_1 = \theta' \text{ and } \theta_2 = \theta_1' \quad (24)$$

$$\theta_2 = \theta_1' = \frac{1}{1 + \frac{4}{3} Rd} \left[ \text{Pr} \left( \frac{A_0}{A_4} \text{Ec} (f_2)^2 + \frac{A_2}{A_4} \text{Ec} M (E_1 - f_1)^2 + \frac{A_3}{A_4} f \theta_1 \left( \frac{1-n}{1+n} \right) \right) \right] \quad (25)$$

Along with boundary conditions, where:

$$f(\eta) = \left( \frac{1-n}{1+n} \right) \alpha, f'(\eta) = 1, \theta'(\eta) = -\delta(1-\theta(0)) \text{ at } \eta = 0 \text{ and } f'(\eta) = 0, \theta(\eta) = 0, \eta \rightarrow \infty$$

where

$$A_0 = \frac{\mu_{nf}}{\mu_f} = \frac{1}{(1-\phi)^{2.5}} \quad (26)$$

$$A_1 = \frac{\rho_{nf}}{\rho_f} = (1-\phi)\rho_f + \phi \frac{\rho_p}{\rho_f} \quad (27)$$

$$A_2 = \frac{\sigma_{nf}}{\sigma_f} = 1 + \frac{3\phi \left( \frac{\sigma_p}{\sigma_f} - 1 \right)}{\left( \frac{\sigma_p}{\sigma_f} + 2 \right) - \left( \frac{\sigma_p}{\sigma_f} - 1 \right) \phi} \quad (28)$$

$$A_3 = \frac{(\rho C_p)_{nf}}{(\rho C_p)_f} = (1-\phi) + \phi \frac{(\rho C_p)_s}{(\rho C_p)_f} \quad (29)$$

$$A_4 = \frac{k_{nf}}{k_f} = \frac{(k_s + 2k_f) - 2\phi(k_f - k_s)}{(k_s + 2k_f) + \phi(k_f - k_s)} \quad (30)$$

The differential operator is defined by:

$$\frac{df}{d\eta} = q(\eta, f), f(\eta_0) = f_0 \quad (31)$$

$$\frac{d\theta}{d\eta} = q(\eta, \theta), \theta(\eta_0) = \theta_0 \quad (32)$$

The formula for Adam-Bashforth predictor approach is given by:

$$f_{k+1} = f_k + \frac{3h}{2} q(\eta_k, f_k) - \frac{h}{2} q(\eta_{k-1}, f_{k-1}) \quad (33)$$

$$\theta_{k+1} = \theta_k + \frac{3h}{2} q(\eta_k, \theta_k) - \frac{h}{2} q(\eta_{k-1}, \theta_{k-1}) \quad (34)$$

whereas Adam-Malton formula is:

$$f_{k+1} = f_k + \frac{h}{2} q(\eta_{k+1}, f_{k+1}) - \frac{h}{2} q(\eta_k, f_k) \quad (35)$$

$$\theta_{k+1} = \theta_k + \frac{h}{2} q(\eta_{k+1}, \theta_{k+1}) - \frac{h}{2} q(\eta_k, \theta_k) \quad (36)$$

where  $h$  is step size.

The obtained results were verified and compared with previous analysis.

### Analysis of results

The effect of various physical parameters is depicted graphically. The parameters taken into consideration are heat generation or absorption factor, the thickness of wall, electric and magnetic field factors, viscous dissipation. Table 2 is proposed to compare the results with previous studies. The results obtained are in good agreement with earlier stability analysis. The elongated surface's conduct is determined by changes in the VPI, or  $n$ . Figure 2(a) and 2(b) illustrate how the value of  $n$  affects the temperature and velocity curves. The stretching velocity rises as the value of  $n$  grows, causing more fluid to be distorted and an increase in the velocity boundary-layer. The increase in velocity reduces heat carrying phenomenon.

**Table 2. Comparison of results with previous studies**

| Pr  | Gul <i>et al.</i> [8] | Saeed <i>et al.</i> [9] | Present study |
|-----|-----------------------|-------------------------|---------------|
| 2   | 0.9113                | 0.9114                  | 0.9110        |
| 6.2 | 1.5797                | 1.5796                  | 1.5786        |
| 7   | 1.8954                | 1.8954                  | 1.8964        |
| 20  | 1.3539                | 1.3539                  | 1.3539        |

The velocity gradient is significantly reduced when fluid is nearer to sheet, leading to reduction in boundary-layer. Because of the wall thickness parameter, the temperature gradient likewise exhibits a falling tendency. Figure 3 illustrates how the magnetic factor affects both the temperature gradient and speed. Increase in magnetic field decreases movement of nanofluid. This is obvious as increase in value of MHD on electrically charged nanoparticles leads to rise in Lorentz force, a force which resists movement of fluid. This property can be used to get desired velocity. The graph illustrates how the magnetic field is inversely related to velocity.

Figure 4 shows how viscous dissipation affects temperature. Eckert number shows relation between the kinetic energy of nanofluid-flow and the enthalpy discrepancy between the surrounding area and the wall which represents heat dissipation. Dimensionless temperature for various,  $Rd$ , values is also displayed in fig. 4. The radiation parameter is designed to detect rate of heat transfer. As increase in radiation accelerates amount of heat transfer which leads to increase in boundary-layer thickness, therefore both temperature gradient and boundary-layer pick up higher values by increasing  $Rd$ . Radiation effect is designed to estimate velocity of fluid.

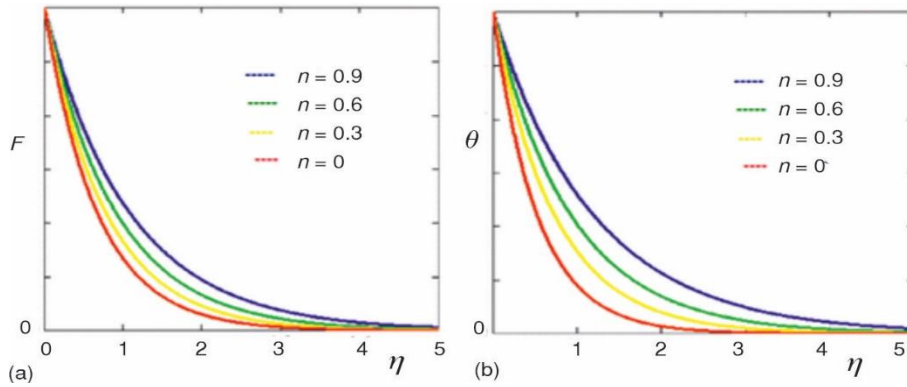


Figure 2. Effect of  $n$ ; (a) temperature and (b) velocity

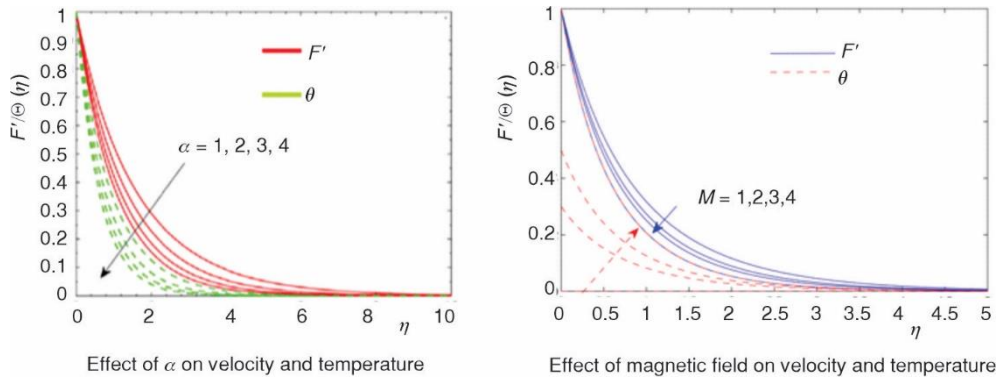


Figure 3. Velocity and temperature difference of magnetic field

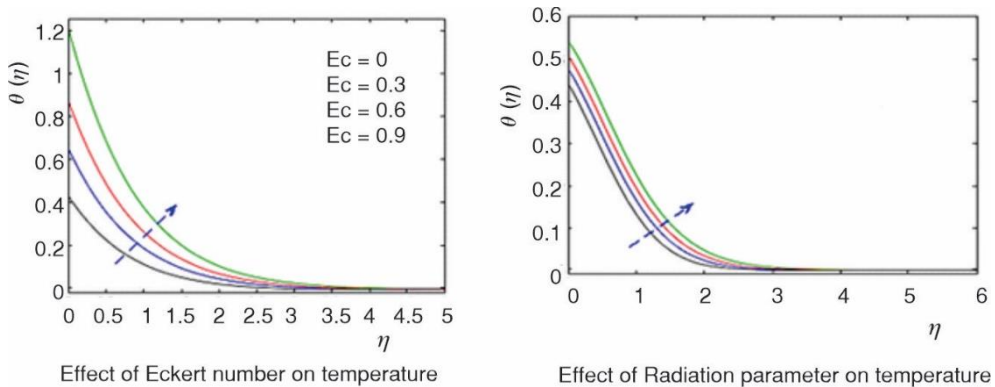
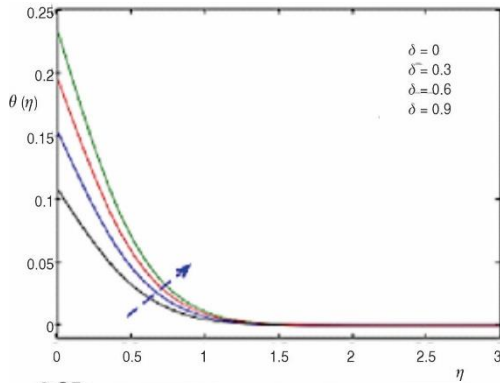


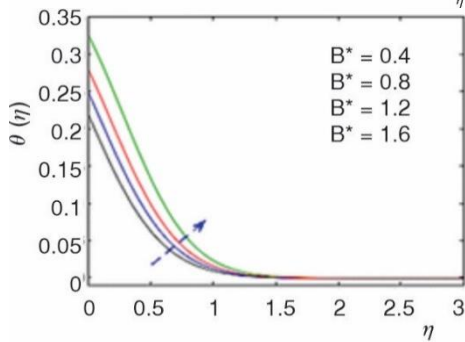
Figure 4. Temperature effect of Eckert number and radiation parameter

Figure 5 illustrates the impact of Biot number,  $\delta$ . The ratio of convection of thermal transmission by conduction of thermal transmission is known as the Biot number, and it plays a role in the boundary conditions.

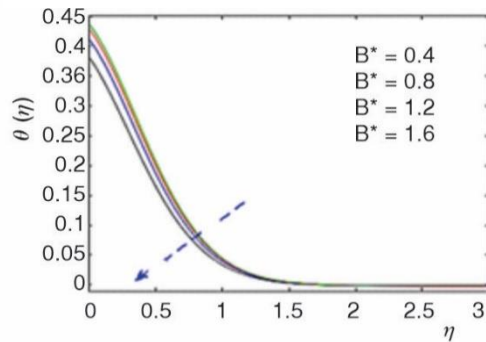
The effect of the heat generation or absorption factor,  $A^*$ , which is dependent on space is noticeable in fig 6. It was revealed that the dispersion of heat releases energy, which causes the temperature gradient to be bigger since the values of  $A^*$  are enhanced.



**Figure 5. Influence of Boit number on temperature**

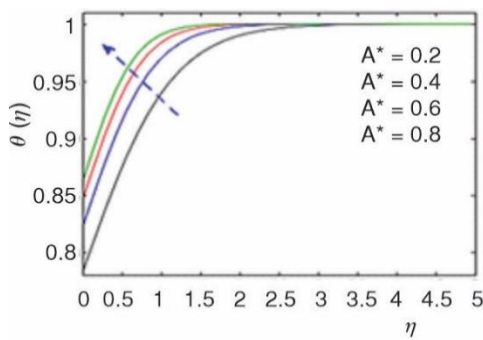


Effect of positive  $B^*$  on temperature

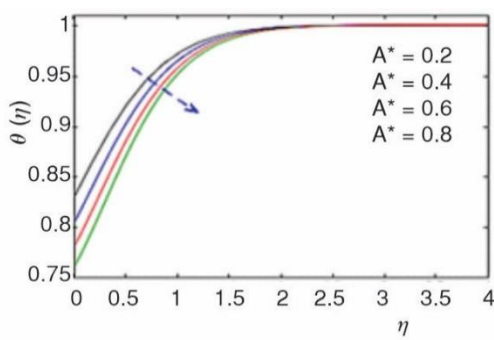


Effect of negative  $B^*$  on temperature

**Figure 6. Positive and negative results of temperature**



Effect of positive  $A^*$  on temperature



Effect of negative  $A^*$  on temperature

**Figure 7. Heat absorption or generation factor on temperature**

The impact of a heat absorption or generation factor on temperature is shown in fig. 7. The graphs indicates that increment in values of  $B^*$  increases the temperature gradient. It is also found that for negative values of  $B^*$  more heat is absorbed reducing value of temperature gradient.

### Conclusions

The current work focuses on a 2-D elongated surface with varying thickness nanofluid EMHD flow. A survey has been conducted on the effects of an electrically charged particle-

filled magnetic field on heat flux values, fluid with varied viscosity, and so on an extended surface with varying thickness. Using similarity transformations, the PDE are transformed into ODE ones, and the non-dimensionalization of the variables is solved numerically. A diagrammatic depiction of the temperature and velocity profile was used to examine the results of several physical variables. The following are the main results from this investigation:

- When the power index of velocity rises, both the fluid's velocity and the nanofluid's temperature accelerate.
- As a result of increasing the wall width factor, the temperature and velocity of the fluid both drop.
- The fluid velocity and Hartmann number both decrease with temperature.
- The fluid's temperature rises when the heat transfer is increased, as shown by increases in the factor of heat radiation, viscous dissipation, and Biot number.
- For the positive values increment, the effect of the time dependent and space-dependent absorption and generation of heat parameter produces heat and reduces temperature when the negative values reduces.

### Nomenclature

|            |   |
|------------|---|
| $A$        | – variable viscosity parameter                          |
| $A^*$      | – space-dependent co-efficient                          |
| $B^*$      | – time-dependent co-efficient                           |
| $B_0$      | – magnetic field strength, [T]                          |
| $C_p$      | – heat capacity, [ $\text{Jkg}^{-1}\text{K}^{-1}$ ]     |
| $E_0$      | – electric field strength, [ $\text{NC}^{-1}$ ]         |
| $E_1$      | – electric field parameter                              |
| $Ec$       | – Eckert number   |
| $k^*$      | – mean absorption coefficient                           |
| $M$        | – magnetic field parameter                              |
| $N$        | – co-efficient related to stretching sheet              |
| $n$        | – parameter of velocity power index                     |
| $Pr$       | – Prandtl number  |
| $q_r$      | – radiative heat flux, [ $\text{Wm}^{-2}$ ]             |
| $Rd$       | – parameter of radiation                                |
| $T$        | – fluid temperature, [K]                                |
| $T_w$      | – wall temperature, [K]                                 |
| $T_\infty$ | – free stream temperature, [K]                          |
| $U_w$      | – velocity of fluid at Stretching, [ $\text{ms}^{-1}$ ] |

$u, v$  – components of velocity along  
x- and y-axis, [ $\text{ms}^{-1}$ ]

### Greek symbols

|            |  |
|------------|--|
| $\alpha$   | – wall thickness parameter                                     |
| $\delta$   | – Biot number  |
| $\eta$     | – non-dimensional similarity variable                          |
| $\theta$   | – dimensionless temperature, [K]                               |
| $\kappa$   | – thermal conductivity [ $\text{Wm}^{-1}\text{K}^{-1}$ ]       |
| $\mu$      | – dynamic viscosity [ $\text{kgm}^{-1}\text{s}^{-1}$ ]         |
| $\nu$      | – kinematic viscosity, [ $\text{m}^2\text{s}^{-1}$ ]           |
| $\rho$     | – density, [ $\text{kgm}^{-3}$ ]                               |
| $\sigma$   | – electric conductivity, [ $\text{Sm}^{-1}$ ]                  |
| $\sigma^*$ | – Stefan–Boltzmann constant, [ $\text{Wm}^{-2}\text{K}^{-4}$ ] |

### Subscripts

|    |              |
|----|--------------|
| f  | – base fluid |
| nf | – nanofluid  |

### References

- [1] Khan, W. A., Pop, I., Boundary-Layer Flow of a Nanofluid Past a Stretching Sheet, *Inter. Jour. Heat Mass Transfer*, 53, (2010), 11-12, pp. 2477-2483
- [2] Ibrahim, W., Shankar, B., MHD Boundary-Layer Flow and Heat Transfer of a Nanofluid Past a Permeable Stretching Sheet with Velocity, Thermal and Solutal Slip Boundary Conditions, *Com. and Fluids*, 75 (2013), Apr., pp. 1-10
- [3] Gireesha, B., *et al.*, Flow of Hybrid Nanofluid Across a Permeable Longitudinal Moving Fin Along with Thermal Radiation and Natural Convection, *Com. Methods and Programs in Biomed.* 185 (2020), 105166
- [4] Makarem, M. A., *et al.*, A Numerical Investigation on the Heat and Fluid-Flow of Various Nanofluids on a Stretching Sheet, *Heat Transfer Asian Research*, 47 (2018), 2, pp. 347-365
- [5] Ghalambaz, M., *et al.*, Mixed Convection Boundary-Layer Flow and Heat Transfer Over a Vertical Plate Embedded in a Porous Medium Filled with a Suspension of Nano-Encapsulated Phase Change Materials, *Jo. of Molecular Liquid*, 293, (2019), 111432

- [6] Wakif, A., Sehaqui, R., Generalized Differential Quadrature Scrutinization of an Advanced MHD Stability Problem Concerned Water-Based Nanofluids with Metal/Metal Oxide Nanomaterials: A Proper Application of the Revised Two-Phase Nanofluid Model with Convective Heating and Through-Flow Boundary Conditions, *Numerical Methods for Partial Differential Equations*, 38 (2020), 3, pp. 608-635
- [7] Hajjar, A., *et al.*, Time Periodic Natural Convection Heat Transfer in a Nano-Encapsulated Phase-Change Suspension, *Intern. Journ. Mech. Sci.*, 166, (2020), 105243
- [8] Gul, T., *et al.*, Magnetohydrodynamic Impact on Carreau Thin Film Couple Stress Nanofluid-flow over an Unsteady Stretching Sheet, *Math. Probs. in Eng.*, 16 (2021), 8003805
- [9] Saeed, A., *et al.*, Non-linear Convective Flow of the Thin Film Nanofluid Over an Inclined Stretching Surface, *Sci. Repts.*, 11, (2021), 18410
- [10] Mathew, A., *et al.*, Significance of Multiple Slip and Nanoparticle Shape on Stagnation Point Flow of Silver-Blood Nanofluid in the Presence of Induced Magnetic Field, *Surf and Interfaces*, 25 (2021), 101267
- [11] Krishnamurthy, M., *et al.*, Effect of Viscous Dissipation on Hydromagnetic Fluid-Flow and Heat Transfer of Nanofluid Over an Exponentially Stretching Sheet with Fluid-Particle Suspension, *Cogent Math.* 2, (2015), 1, 1050973
- [12] Senthilraja, S., *et al.*, A Comparative Study on Thermal Conductivity of  $\text{Al}_2\text{O}_3/\text{Water}$ ,  $\text{CuO}/\text{Water}$  and  $\text{Al}_2\text{O}_3\text{-CuO}/\text{Water}$  Nanofluids, *Digest Journal Nanomaterials Biostructures*, 10, (2015), 4, pp. 1449-1458
- [13] Chamkha, A., *et al.*, Phase-Change Heat Transfer of Single/Hybrid Nanoparticles enhanced Phase-Change Materials Over a Heated Horizontal Cylinder Confined in a Square Cavity, *Advan Powder Tech.*, 28, (2017), 2, pp. 385-397
- [14] Gireesha, B., *et al.*, Flow of Hybrid Nanofluid Across a Permeable Longitudinal Moving Fin Along with Thermal Radiation and Natural Convection, *Com. Meth. and Prog. in Biomed.*, 185, (2020), 105166
- [15] Gopal, D., *et al.*, Numerical Analysis of Higher Order Chemical Reaction on Electrically MHD Nanofluid Under Influence of Viscous Dissipation, *Alexandria Engineering Journal* 60 (2021), 1, pp. 1861-1871
- [16] Sowmya, G., *et al.*, Analysis of a Fully Wetted Moving Fin with Temperature-Dependent Internal Heat Generation Using the Finite Element Method, *Heat Transfer*, 49 (2020), 4, pp. 1939-1954
- [17] Alsaedi, A., *et al.*, Eyring-Powell Nanofluid-Flow with Nonlinear Mixed Convection: Entropy Generation Minimization, *Com. Meth. and Prog. in Biomed.*, 186 (2020), 105183
- [18] Fang, T., *et al.*, Boundary-Layer Flow Over a Stretching Sheet with Variable Thickness, *App. Math.s & Com.*, 218, (2012), 13, pp. 7241-7252
- [19] Khader, M. M., Megahed, A. M., Numerical Solution for Boundary-Layer Flow Due to a Nonlinearly Stretching Sheet with Variable Thickness and Slip Velocity, *Eur. Phyl. Journal Plus*, 128 (2013), Sept., 100
- [20] Alawi, O.A., *et al.*, Thermal Conductivity and Viscosity Models of Metallic Oxides Nanofluids, *Intern. J. of Heat and Mass Transfer.*, 116, (2018), Jan., pp. 1314-1325
- [21] Suresh, S., *et al.*, Effect of  $\text{Al}_2\text{O}_3\text{-Cu}/\text{Water}$  Hybrid Nanofluid in Heat Transfer, *Experimental Thermal and Fluid Science* 2012 (2021), 38, pp. 54-60
- [22] Momin, G. C., Experimental Investigation of Mixed Convection with Water- $\text{Al}_2\text{O}_3$  & Hybrid Nanofluid in Inclined Tube for Laminar Flow, *Inter. J. of Sci. and Tech. Research*, 2 (2013), 2, pp. 195-202
- [23] Takabi, B., Salehi, S., Augmentation of the Heat Transfer Performance of a Sinusoidal Corrugated Enclosure by Employing Hybrid Nanofluid, *Advances in Mechanical Engineering*, 6 (2014), 147059
- [24] Devi, S. P. A., Devi, S. S. U., Numerical Investigation of Hydromagnetic Hybrid  $\text{Cu-Al}_2\text{O}_3/\text{Water}$  Nanofluid-Flow Over a Permeable stretching Sheet With Suction, *Inter. J. of Nonlinear Sci. and Numerical Simulation.*, 17, (2016), 5, pp. 249-257
- [25] Ghalambaz, M., *et al.*, Phase-Change Heat Transfer in a Cavity Heated From Below: The Effect of Utilizing Single or Hybrid Nanoparticles as Additives, *J. of Taiwan Ins. of Che. Eng.*, 72 (2017), Mar., pp. 104-115
- [26] Shuguang, Li., *et al.*, Analysis of the Thomson and Troian Velocity Slip for the Flow of Ternary Nanofluid Past a Stretching Sheet, *Scientific Reports*, 13 (2023), Feb., pp. 2340-2351

- [27] Vishalkumar, J. P., Meher, R., Analysis of MHD tangent Hyperbolic Hybrid Nanofluid-Flow with Different Base Fluids over a Porous Stretched Sheet, *Journal of Taibah University for Science*, 18 (2024), 1, pp. 1239-1252
- [28] Suresh, S., *et al.*, Effect of Al<sub>2</sub>O<sub>3</sub>-Cu/Water Hybrid Nanofluid in Heat Transfer, *Experimental Thermal and Fluid Science*, 38 (2012), Apr., pp. 54-60
- [29] Ibrahim, W., Shankar, B., MHD Boundary-Layer Flow and Heat Transfer of a Nanofluid Past a Permeable Stretching Sheet with Velocity, Thermal and Solutal Slip Boundary Conditions, *Computers and Fluids*, 75, (2013), Apr., pp. 1-10